



**HAL**  
open science

## Field-induced layering of confined ferromagnetic nanoparticles: The role of attractive interactions

Jelena Jordanovic, Sabine Hl Klapp

► **To cite this version:**

Jelena Jordanovic, Sabine Hl Klapp. Field-induced layering of confined ferromagnetic nanoparticles: The role of attractive interactions. *Molecular Physics*, 2009, 107 (04-06), pp.599-607. 10.1080/00268970902889634 . hal-00513283

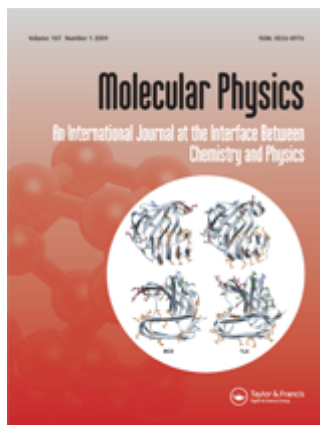
**HAL Id: hal-00513283**

**<https://hal.science/hal-00513283>**

Submitted on 1 Sep 2010

**HAL** is a multi-disciplinary open access archive for the deposit and dissemination of scientific research documents, whether they are published or not. The documents may come from teaching and research institutions in France or abroad, or from public or private research centers.

L'archive ouverte pluridisciplinaire **HAL**, est destinée au dépôt et à la diffusion de documents scientifiques de niveau recherche, publiés ou non, émanant des établissements d'enseignement et de recherche français ou étrangers, des laboratoires publics ou privés.



**Field-induced layering of confined ferromagnetic nanoparticles: The role of attractive interactions**

Journal:	<i>Molecular Physics</i>
Manuscript ID:	TMPH-2008-0442.R1
Manuscript Type:	Special Issue Paper - Dr. Jean-Jacques Weis
Date Submitted by the Author:	06-Mar-2009
Complete List of Authors:	Jordanovic, Jelena; Free University Berlin, Department of Physics, Institute of Theoretical Physics Klapp, Sabine; Free University Berlin, Department of Physics, Institute of Theoretical Physics
Keywords:	computer simulations, dipolar fluids, nanoparticles, magnetic fields
<p>Note: The following files were submitted by the author for peer review, but cannot be converted to PDF. You must view these files (e.g. movies) online.</p> <p>manuscript_2.tex</p>	



# Field-induced layering of confined ferromagnetic nanoparticles: The role of attractive interactions

JELENA JORDANOVIC and SABINE H. L. KLAPP\*

*Institute of Theoretical Physics, Dept. of Physics,  
Freie Universität Berlin, Arnimallee 14, 14195 Berlin, Germany*

(Dated: March 6, 2009)

## Abstract

We present Molecular Dynamics simulation results for confined ferromagnetic nanoparticles (film geometry) under the influence of strong, homogeneous magnetic fields. We focus on the role of short-ranged attractive interactions between the particles for the structure formation in thin films consisting of four to five monolayers. To this end we compare simulation results for Stockmayer particles (Lennard-Jones plus dipolar interactions) with corresponding results for dipolar soft spheres, where the short-ranged potential is purely repulsive. At moderate and large average densities, both systems exhibit pronounced layering. Based on the corresponding normal pressure oscillations we show that the field-induced effects on the layer formation in this density range are essentially independent of the short-range interactions. The dipolar soft sphere system merely has a stronger tendency to form a crystal-like lateral structure upon application of a parallel field. More pronounced differences occur at lower densities and not too high dipolar coupling strengths within the vapor-liquid region of the confined, zero-field Stockmayer system. Applying a perpendicular field, the Stockmayer system develops a blob structure absent in the corresponding repulsive system. Finally, for very large values of both, dipolar coupling parameter and field strength of a perpendicular field, we find evidence for a field-induced in-plane crystallization of the layered systems.

---

\*Corresponding author. Email: klapp@physik.fu-berlin.de

## I. INTRODUCTION

Within the last years the self-organization of magnetic nanoparticles at interfaces has become a focus of growing interest. Even without an external (magnetic) field, particles with sufficiently strong magnetic dipole moments aggregate into in-plane chains and networks, when confined to surfaces or thin films [1, 2]. Additional phenomena emerge when magnetic nanoparticle systems are subject to an external magnetic field directed parallel or perpendicular to the interface. Here one observes the formation of mesoscopic patterns such as labyrinths and void structures. **Such pattern formation has been observed, e.g., in experiments of ferromagnetic films [3] and in theoretical [4] and combined theoretical-experimental studies of magnetic nanocrystals [5, 6].** Similar behavior is seen in systems of superparamagnetic particles [7, 8] or polarizable particles [9] where external fields trigger crystallization and other patterns. Moreover, extending the systems somewhat into the third dimension the lateral structures are supplemented by structure formation in vertical direction such as layering. **This has been shown in recent experiments of ferrofluids [10] and related computer simulation studies [11, 12].**

For a precise *control* of these structures a detailed understanding of the impact of the underlying microscopic interactions is inevitable. Indeed, while it is clear that dipole-dipole and dipole-field interactions play a key role for the pattern formation, less is known about the impact of the short-ranged forces between the nanoparticles. An important example is the van-der-Waals attraction stemming from the charge density fluctuations within the particles and the resulting induced dipolar interactions. The van-der-Waals interaction can be experimentally tuned, e.g., by varying the thickness of the surfactant layer. In a recent combined experimental-theoretical study, Lalatonne *et al.* [6, 13] have explored the role of such attractive interactions on the pattern formation of magnetic nanocrystals in parallel fields. It was demonstrated that pattern formation (such as stripes) only occurs in systems where the dipole-dipole interactions are supplemented by van-der-Waals forces. In a subsequent computer simulation study, Richardi *et al.* [14] considered film-like systems in perpendicular magnetic fields. The particles were modelled via the Stockmayer (SM) potential including an attractive (van-der-Waals-like) contribution on top of the dipole-dipole interaction and steric repulsion. The resulting system displays a variety of structures at thermodynamic conditions where the zero-field, confined SM fluid was within a two-phase

1  
2  
3 region of its vapor-liquid transition [14]. Finally, a simulation study of Ilg [15] revealed the  
4 importance of attractive depletion interactions on the field-induced local, hexagonal ordering  
5 in three-dimensional ferrofluids [1, 2].  
6  
7

8  
9 Motivated by these findings we investigate in the present paper the role of attractive in-  
10 teractions for field-induced layering effects in dipolar nanofilms. Indeed, as we have recently  
11 demonstrated via Molecular Dynamics (MD) simulations for confined SM particles [11, 12],  
12 external (homogeneous) magnetic fields directed parallel or perpendicular to the confining  
13 surfaces can "trigger" the formation or destruction of layers present in zero field. The surface  
14 separations where this becomes possible can be inferred from the location of maxima and  
15 minima of the normal pressure as function of the wall separation [11]. We also observed [12]  
16 interesting structure formation within the layers such as a hexagonal-like ordering in dense  
17 systems subject to parallel fields.  
18  
19

20  
21 To explore the role of attractive interactions we compare in this study MD results for  
22 the field-induced behavior of confined Stockmayer fluids with those for dipolar soft sphere  
23 (DSS) systems where the attractive part of the spherical potential is entirely missing. We  
24 specialize on nanoconfined systems where the film thickness is only a few particle diameters.  
25  
26

27  
28 The remainder of the paper is organized as follows. In section II we introduce the model  
29 systems and the corresponding simulation parameters. Numerical results are presented in  
30 section III, and in section IV we give some conclusions.  
31  
32

## 33 II. MODEL SYSTEM

34  
35 Our model fluid consists of spherical particles (diameter  $\sigma$ ) with three-dimensional, per-  
36 manent point dipole moments  $\boldsymbol{\mu}_i$  ( $i = 1, \dots, N$ ). The particles interact via the pair potential  
37  
38

$$39 \quad u_{\text{FF}}(ij) = 4\epsilon \left[ \left( \frac{\sigma}{r_{ij}} \right)^{12} - \kappa \left( \frac{\sigma}{r_{ij}} \right)^6 \right] + \left[ \frac{\boldsymbol{\mu}_i \cdot \boldsymbol{\mu}_j}{r_{ij}^3} - 3 \frac{(\boldsymbol{\mu}_i \cdot \mathbf{r}_{ij})(\boldsymbol{\mu}_j \cdot \mathbf{r}_{ij})}{r_{ij}^5} \right], \quad (2.1)$$

40  
41 where  $r_{ij} = |\mathbf{r}_{ij}| = |\mathbf{r}_i - \mathbf{r}_j|$  is the separation of two particles  $i$  and  $j$ . The parameter  $\kappa$   
42 controls the strength of the isotropic, van-der-Waals-like attraction between the particles.  
43 For  $\kappa = 1$  the interaction potential (2.1) corresponds to that of a SM fluid, whereas the case  
44  $\kappa = 0$  describes a DSS fluid. Following previous work [12, 16] we use a truncated and shifted  
45 version of the short-ranged potential.  
46  
47  
48  
49  
50  
51  
52  
53  
54  
55  
56  
57  
58

59 To model a fluid film we introduce two plane-parallel walls located at  $z = \pm L_z/2$ , which  
60

are infinitely extended in the  $x$ - $y$  plane. The fluid-wall potentials affecting particle  $i$  are given by

$$u_{\text{FW}}^{\pm}(i) = \frac{2\pi}{3}\epsilon \left[ \frac{2}{15} \left( \frac{\sigma}{L_z/2 \pm z_i} \right)^9 - \kappa \left( \frac{\sigma}{L_z/2 \pm z_i} \right)^3 \right], \quad (2.2)$$

where the minus (plus) corresponds to the interaction with the upper (lower) wall. **For simplicity (and to be consistent with our earlier work on SM systems [11, 12])** the attractive contribution of the fluid-wall potential is controlled by the *same* parameter  $\kappa$  appearing in the fluid-fluid interaction (2.1). **In other words, the SM particles ( $\kappa = 1$ ) are subject to attractive walls, whereas the DSS system ( $\kappa = 0$ ) is considered with repulsive walls. Clearly, this choice is somewhat arbitrary. However, performing test calculations with the "opposite" model, that is, SM (DSS) particles between repulsive (attractive) walls, we have found that the presence or absence of fluid-wall attraction does not significantly influence our results (contrary to the attractive term in the fluid-fluid interaction).**

Finally, the particles are subject to an external, homogeneous field  $\mathbf{H}$ , yielding a potential contribution

$$u_{\text{DF}}(i) = -\boldsymbol{\mu}_i \cdot \mathbf{H}. \quad (2.3)$$

The external field is directed either perpendicular to the surfaces, i.e.,  $\mathbf{H} = \mathbf{H}_z = H_z \hat{\mathbf{e}}_z$ , or parallel to an (arbitrary) axis with the plane, i.e.,  $\mathbf{H} = \mathbf{H}_{\parallel} = H_{\parallel} \hat{\mathbf{e}}_{\alpha}$  (with  $\hat{\mathbf{e}}_{\alpha}$  being the unity vector in direction  $\alpha$ ).

The calculations were performed via MD simulations of  $N = 500$  particles at constant (kinetic) temperature  $T$  [17]. Technical details can be found elsewhere [16]. The simulations were carried out at the reduced temperature  $T^* = k_{\text{B}}T/\epsilon = 1.35$  and reduced densities  $\rho^* = \rho\sigma^3 = N\sigma^3/AL_z$  (with  $A$  being the lateral area of the simulation box) between 0.2 and 0.8. The reduced dipole moments  $\mu^* = \mu/\sqrt{\epsilon\sigma^3}$  were set to values between 2.0 and 5.2, corresponding to dipolar coupling parameters  $\lambda = \mu^2/k_{\text{B}}T\sigma^3 = (\mu^*)^2/T^*$  in the range 3 to 20. We focussed on nanoconfined systems characterized by the wall separation  $L_z^* = L_z/\sigma = 5.0$ , and strong external fields described by reduced field strengths  $H^* = H\mu/k_{\text{B}}T \lesssim 105$ . These values were chosen to be consistent with earlier work by us [11, 12].

FIG. 1:

### III. RESULTS

#### A. Layering effects

We start by investigating the impact of the attractive interactions on the field-induced layering occurring in relatively dense fluids close to surfaces. We note that layering itself is a rather typical phenomenon of nanoconfined fluids and as such not specific for dipolar (magnetic) systems (see, e.g., [18]). The particular feature of dipolar particles, as we have demonstrated before [11], is that external perpendicular fields can trigger formation of additional layers which are absent in zero field. Likewise, external parallel fields can destroy layers. A convenient indicator for these effects is the normal pressure [18] at zero field,

$$P_z = -\frac{1}{A} \frac{\partial \mathcal{F}}{\partial L_z} = k_B T \left( \frac{N}{AL_z} - \frac{1}{A} \left\langle \frac{\partial H^{\text{pot}}}{\partial L_z} \right\rangle \right), \quad (3.1)$$

where  $\mathcal{F}$  is the free energy and  $H^{\text{pot}}$  is the total potential Hamilton function of the system involving both, fluid-fluid and fluid-wall interactions (see equations (2.1) and (2.2), respectively). The function  $P_z(L_z)$  is directly related to the solvation force measurable in surface-force experiments [18, 19]. Typical zero-field results for the reduced pressure  $P_z^* = P_z \sigma^3 / \epsilon$  in the SM and DSS systems at three different average densities are plotted in figure 1. We focus on a range of separations  $L_z^*$  allowing the system to form three to five layers (depending on  $\rho^*$ ) in zero field. The transition between these ranges is indicated by oscillations in  $P_z^*(L_z^*)$ , which are typical of nanoconfined fluids [18]. For the particular case of dense SM fluids we have already shown via an analysis of density profiles [11] that the location of the minima (maxima) of  $P_z^*(L_z^*)$  indicates those separations where an external perpendicular (parallel) field can create (destroy) a layer. This is consistent with the common picture [18] that a minimum of  $P_z^*(L_z^*)$  reflects a "comfortable" arrangement of the confined particles, which allows for some compression in vertical direction. Likewise, a maximum indicates a high tendency of the system to release pressure.

Comparing now the pressure data for SM and DSS fluids (see figure 1) we observe, on one hand, large differences regarding the actual numerical values for  $P_z^*$  at given  $L_z^*$  for all densities considered. These differences signal a higher overall repulsion in the DSS system,

FIG. 2:

FIG. 3:

as expected in view of the missing attractive contributions to the fluid-fluid and fluid-wall potentials (see equations (2.1) and (2.2) with  $\kappa = 0$ ). On the other hand, the *location* of the maxima and minima for the denser systems is nearly identical, as can be seen from figures 1 (a) and (b) for  $\rho^* = 0.6$ , and from figures 1 (d), and (e) for  $\rho^* = 0.8$ . We therefore expect that an external field will have the same impact on the number of layers regardless of the attractive interactions. That this is indeed the case can be checked via the density profiles  $\rho(z)$ . A typical example is presented in figure 2 where we show results obtained at  $\rho^* = 0.8$  and  $L_z^* = 5.0$ . In zero field, both the SM and the DSS system are characterized by five well-pronounced layers, and the normal pressure is in a maximum (see figures 1(a) and (d)). The maximum indicates that an external parallel field can destroy one layer, as seen explicitly from the corresponding density profiles at  $H_{\parallel}^* = 74$  included in figure 2. Closer inspection reveals some differences between the two models concerning to the degree of stratification. Indeed, already in zero field the DSS system (see figure 2(b)) is characterized by a nearly solid-like translational structure normal to the walls, i.e.,  $\rho(z)$  is essentially zero between the peaks. In the strong parallel field the DSS system then develops a small density "spike" between the two inner peaks, which is absent in the SM system (see figure 2(a)) and indicates a somehow imperfect arrangement of the layers. These differences are accompanied by differences in the lateral structure. The latter can be measured by in-plane ("intra-layer") correlation functions and inter-layer correlations functions,  $g^{\text{intra}}(R)$  and  $g^{\text{inter}}(R)$ , respectively (with  $R = \sqrt{\Delta x^2 + \Delta y^2}$  being the lateral separation) [12]. Results for the correlation functions are shown in figure 3, where we focus on the contact layer next to the walls and correlations between contact and the next inner layer. In both model systems, application of the parallel field significantly enhances the degree of short-range correlations. In particular, the asymmetric peak shapes and the onset of a splitting of the second-peak reflect a field-induced *hexagonal* ordering of the particles both within and in between neighboring layers. Interestingly, these effects are even more pronounced in the

FIG. 4:

DSS system (see figure 3(b)), indicating that the absence of attraction supports the system in developing translational order. In terms of the hexagonal bond-order parameter  $\Psi_6$  [12], however, DSS and SM fluids behave again very similar: both systems are characterized by rather large values of  $\Psi_6 \approx 0.8$  at  $H_{\parallel}^* = 74$  as compared to  $\Psi_6 \approx 0.5$  at  $H^* = 0$ . A similar agreement between SM and DSS systems is found with respect to layer formation induced by a perpendicular field at  $\rho^* = 0.8$ , as well as for the somewhat lower average density  $\rho^* = 0.6$  (see the corresponding pressure curves in figures 1 (b) and (e)).

Upon further decrease of  $\rho^*$  already the zero-field layering becomes less pronounced. This is reflected by the softer shape of the curves  $P_z^*(L_z^*)$  at  $\rho^* = 0.4$ , which are plotted in figures 1(c) and (f) for the SM and DSS system, respectively. The slightly negative values of  $P_z^*$  in the SM case (which are accompanied by similar values of the parallel pressure) arise since this fluid is presumably already in or close to the vapor-liquid two-phase region at the density considered (and  $H^* = 0$ ) according to previous simulation studies [14]. We present the results nevertheless, since we are mainly interested in the impact of a perpendicular field. **The latter tends to stabilize the system in the sense that, upon increasing  $H_z^*$ , more and more particles mutually repel each other. This is also indicated by the fact that the normal pressure becomes positive (as does the pressure component parallel to the walls). For example, at  $H_z^* = 74$  we find  $P_z^*(L_z^* = 3.2) = 7.0$  and  $P_z^*(L_z^* = 5.0) = 4.7$  replacing the negative values found in zero field (see figure 1(c)). Further implications of the "stabilizing" impact of a perpendicular field will be discussed in the following Section III B.**

Comparing now the data for SM and DSS fluids at  $\rho^* = 0.4$  we find that, contrary to the behavior at higher densities, the presence or absence of isotropic attraction influences the location of the (now broader) maxima and minima of  $P_z^*(L_z^*)$ . Thus, systems at given  $L_z^*$  behave differently upon application of an external field. An example is given in figure 4. The wall separation is set to  $L_z^* = 5.0$  where both systems form four layers in zero field (see dashed lines in figure 4). In a strong perpendicular field the SM system develops *five* layers, contrary to the DSS system where the density profile just becomes sharper. This model-dependence is consistent with the fact that the separation  $L_z^* = 5.0$  is close to a minimum of the pressure

FIG. 5:

curve of the SM fluid (see figure 1(c)), but not for the DSS system (see figure 1(f)). To complete the picture, the insets in figure 4 include results at the higher density  $\rho^* = 0.6$  and the same wall separation. Under these conditions the external perpendicular field can trigger formation of a new layer independent of the short-range interaction, as already suggested by the oscillations of the corresponding pressure curves (see figures 1(b) and (e)).

### B. Lateral structure at small densities

We now turn to systems at low overall density, taking the case  $\rho^* = 0.2$  as a representative example. Previous simulation studies by Weis and co-workers [14] suggest that the SM system *without* external field is within a vapor-liquid two-phase coexistence region at this rather low density. Their results further reveal that application of a perpendicular field induces patterns such as columns and labyrinths in sufficiently thick films, that is, at  $L_z^* \geq 10$ .

Here we present results for thinner films characterized by  $L_z^* = 5.0$ . Our main question concerns again the influence of attractive spherical interactions. To this end we note that, without the van-der-Waals interactions (that is, in the DSS case), there is no zero-field vapor-liquid condensation even in the limit  $L_z^* \rightarrow \infty$ .

As a starting point we show in figure 5 typical structures of the confined SM and the DSS fluids at two strengths  $H_z^*$  of an external perpendicular field. Visible differences between the two model systems only appear at the lower field strength  $H_z^* = 7$  (see figures 5(a) and (b)). Here, the SM fluid forms a structure characterized by small blobs and holes, which are essentially absent in the corresponding DSS system. Thus, we interpret the inhomogeneous lateral structure of the SM system in the external field as a reminiscence of the zero-field condensation transition, and as such, a result of the attractive fluid-fluid interactions (consistent with earlier findings [13, 14]). **At the larger field strength  $H_z^* = 74$ , on the other hand, the blob-hole structure of the SM system decomposes (i.e., the droplets dissociate), as visible in figure 5(c). A similar effect was reported in earlier simulations of Weis and co-workers involving thin SM films with purely repulsive walls [14]. This indicates that the decrease of the pattern size with**

FIG. 6:

the field strength is a rather typical phenomenon for systems with attractive fluid-fluid interactions. In the DSS system, on the other hand, the structural differences between low and high field are much less pronounced, as revealed by comparing figures 5(b) and (d). Moreover, comparing the snapshots between DSS and SM systems in the high field (see figures 5 (c) and (d)) we observe a rather similar lateral, dissociated structure. We understand this similarity such that in both systems the field-induced repulsive interactions between the aligned particles in each layer dominate the behavior. We also note that, despite of the small overall density considered, the external field induces in both systems significant density oscillations reflecting four layers at  $H_z^* = 74$  (see figures 5 (e) and (f)).

We next investigate the influence of the dipolar coupling strength,  $\lambda = (\mu^*)^2/T^*$ , on the structure observed in a strong perpendicular field. At fixed  $T^* (= 1.35)$ , an increase of  $\lambda$  corresponds to an increase of the dipolar interactions as compared to the attractive (van-der-Waals) part of the LJ potential. **In other words, the SM system resembles more and more the DSS system.**

Typical configurations for values of  $\lambda$  between 1 and 20 are shown in figure 6. The SM system at  $\lambda = 1$  (see figure 6(a)) displays a blob-hole structure similar to the one already observed at somewhat larger coupling and lower field strength (see figure 5). The physical origin is indeed the same: the blobs are a remainder of an underlying vapor-liquid transition of the same system at  $H^* = 0$ . We note that there are, so far, no simulation results for the vapor-liquid critical point of the confined SM fluid at  $\lambda = 1$  and  $L_z^* = 5$ . However, given the behavior of the same system at  $\lambda \approx 3$  [14], we expect the coexistence region at  $\lambda = 1$  to be even broader. Upon increasing the parameter  $\lambda$  we observe from figures 6 that the configurations characterizing the SM and DSS systems become more and more similar, as expected due to the diminishing role of the van-der-Waals interactions in the SM fluid. A further effect of an increase of  $\lambda$  is that the particles form pronounced chains in vertical direction, i.e., along the field. This feature is even more evident from the correlation functions plotted in figures 7 and 8 for the SM and the DSS system, respectively.

1  
2  
3  
4  
5  
6  
7  
8  
9  
10  
11  
12  
13  
14  
15  
16  
17  
18  
19  
20  
21  
22  
23  
24  
25  
26  
27  
28  
29  
30  
31  
32  
33  
34  
35  
36  
37  
38  
39  
40  
41  
42  
43  
44  
45  
46  
47  
48  
49  
50  
51  
52  
53  
54  
55  
56  
57  
58  
59  
60

FIG. 7:

FIG. 8:

Considering, in particular, the interlayer functions  $g_{12}^{\text{inter}}(R)$  between the contact layer and the next inner layer we observe the development of huge peaks at  $R \approx 0$ , indicating a very high probability of the particles to "sit" on top of each other (see, in particular, figures 7(c) and 8(c)). The formation of vertical chains seems indeed plausible in view of the highly directional character of the dipolar interactions, which favor head-tail alignment. On the other hand, such chains are essentially absent in denser systems [11, 12] where, instead, zig-zag pattern are formed.

Apart from the (vertical) chain formation, an increase of  $\lambda$  induces a pronounced increase of the nearest-neighbor distance *within* each layer due the growing repulsion between the aligned particles. This is seen directly from the snapshots in figures 6 (see, in particular, parts (d) and (h)), and also from the intra-layer correlation functions plotted in figures 7(a) and 8(a), respectively. It is interesting to note that the change of  $g^{\text{intra}}(R)$  with  $\lambda$  is actually non-monotonic for smaller values of the coupling strength. Indeed, for both, the SM and the DSS system, the main peak of  $g^{\text{intra}}(R)$  first becomes broader and *decreases* in height upon increasing  $\lambda$  from small values (such as  $\lambda = 1$ ). Further increasing the dipolar coupling parameter we then observe a significant shift of the position of the main peak towards values larger than two particle diameters and, simultaneously, a pronounced increase of its height. The interlayer correlation functions,  $g^{\text{inter}}(R)$ , exactly follow this trend (see figures 7(b) and 8(b)). We note in passing that the strong increase of the lateral nearest-neighbor distance is accompanied by a change from four to five layers (occurring at  $\lambda \approx 7$  and  $\lambda \approx 10$  for the SM and the DSS system, respectively).

Given the pronounced, lateral correlations at  $\lambda = 20$ , it is an important question whether the combination of strong dipolar coupling (i.e., repulsion within a layer) and the external field actually induces *crystal-like* ordering in lateral directions. Indeed, experiments involving mono-layers (i.e., two-dimensional systems) of superparamagnetic colloids in magnetic field perpendicular to the surface have demonstrated the existence of crystalline hexagonal lattice

FIG. 9:

and other highly ordered structures [7, 8]. To check the degree of, specifically, hexagonal or square order we have calculated suitable bond-order parameters  $\Psi_6$  and  $\Psi_4$ , respectively [12]. It turns out that the structures in figure 6, even at the largest  $\lambda$  considered, are *not* related to particularly high values of the bond-order parameters ( $\Psi_6 \approx 0.5$ ,  $\Psi_4 \approx 0.2$  for both, SM and DSS system). Interestingly, however, we have found evidence that nearly-crystalline structures with very large order parameters do arise at even larger field strengths, such as  $H_z^* = 105$ . **This is particularly surprising in view of the fact that the field-induced magnetization,  $M = N^{-1} \sum_{i=1}^N \hat{\mu}_i \cdot \hat{e}_z$ , is only marginally larger as compared to the case  $H_z^* = 74$  considered before. Specifically, we found  $M = 0.97$  at  $H_z^* = 74$  and  $M = 0.98$  at  $H_z^* = 105$ , indicating that the fluctuations of the dipole moments away from the pre-defined field direction are essentially zero already at the somewhat lower field strength. Examples for the nearly-crystalline structures at  $H_z^* = 105$  are shown in figure 9.** The SM system (at  $\rho^* = 0.2$ , see figure 9(a)) forms a well-pronounced hexagonal in-plane structure characterized by  $\Psi_6 \approx 0.9$  (and  $\Psi_4 \approx 0.1$ ). The DSS system at the same density is less ordered (see figure 9(b)). Nevertheless, also in the DSS system a hexagonal structure (with  $\Psi_6 \approx 0.9$ ) emerges at the lower overall density  $\rho^* = 0.1$  (see figure 9(c)). This density dependence seems plausible, since a lower value of  $\rho^*$  implies more space for the (five) layers to form and thus allows for a more perfect in-plane structure.

We note that the simulation results in figure 9 have not (yet) been tested in terms of system size dependence and/or dependence on the box geometry. The latter is square-like in our simulations and, thus, not ideally suited for a hexagonal lattice. Nevertheless, our results concerning the in-plane ordering are, to some extent, consistent with the afore-mentioned experimental studies [7, 8], although these concern true *two-dimensional* systems. In particular, the (in-plane) packing fraction characterizing the SM system shown in figure 9(a) is  $\eta^{\text{layer}} = (\pi/4)N^{\text{layer}}\sigma^3/A\Delta z \approx 0.16$ . The packing fractions where hexagonal order has been observed experimentally [7, 8] are very similar, although the dipolar interaction strength are typically much larger there.

Finally, we briefly comment on the impact of a *parallel* field at small surface separations

FIG. 10:

and low densities. Under such conditions, both SM and DSS systems display pronounced chain formation in lateral directions, as illustrated by corresponding snapshots in figure 10. The main difference consists of the fact that the missing isotropic attraction in the DSS system yields rather isolated chains, whereas the chains in the SM system tend to organize into stripes. Very similar lateral effects have been observed in MC simulations of monolayers of SM and DSS particles [20]. In the present systems characterized by a finite film thickness, we further observe from figure 10(c) some influence of the van-der-Waals interactions on the vertical density profile. **We first note that both model fluids consist of two layers at the field strength considered, although at this wall separation ( $L_z^* = 5.0$ ) more layers are possible (and indeed seen in zero field). This destruction of layers by a parallel field was already reported in our earlier work [11, 12] and can be explained by the fact that the chain-like (i.e., energetically favorable) in-plane configurations allow for more particles in one layer. Comparing now the profiles for the two model systems we see that the two layers are more pronounced and have a larger separation in the SM than in the DSS system. We understand this difference as a combined effect of the presence (absence) of fluid-wall attraction in the SM (DSS) system (see equation (2.2)), on one hand, and a stronger repulsion between the two, laterally structured layers in the SM case, on the other hand.**

#### IV. SUMMARY AND CONCLUSION

In this paper we have employed MD computer simulations to investigate the role of attractive **particle** interactions for the structure formation of thin films of ferrofluids under the influence of external magnetic fields. To this end we have compared results from a SM model, on one hand, and a purely repulsive DSS system, on the other hand. **The fluid-wall potentials have been chosen accordingly (indeed, test calculations show that the details of the fluid-wall potential are essentially unimportant for our results).**

As to the importance of attractive fluid-fluid interactions, we have found that these are mainly relevant at small overall densities. Here, the zero-field SM system

has a vapor-liquid transition, whereas the DSS system has not. In presence of a not too strong perpendicular field, the SM fluid then exhibits a rather inhomogeneous (blob-hole) structure, contrary to the more or less homogeneous distribution of the DSS system. These differences become smaller upon increasing the dipolar coupling parameter (i.e., diminishing the role of the van-der-Waals attraction) and/or increasing the strength of a (perpendicular) external field. Indeed, for very large values of both, dipolar coupling parameter and field strength of a perpendicular field, we find evidence for an in-plane crystallization (into a hexagonal structure) of the layered systems. This finding is particularly interesting in view of the experimental observation of field-induced hexagonal order in *monolayers* of paramagnetic colloids (and similar packing fractions) [7, 8]. It is clear, however, that simulations of larger system sizes (and flexible box geometry) are necessary in order to establish the crystallization in the dipolar model films.

### Acknowledgments

S.H.L.K. would like to thank J.-J. Weis for many stimulating and enlightening discussions on computer simulations of dipolar systems. We also acknowledge financial support from the German Science Foundation via the SFB448 "Mesoscopically structured composites" (project B6).

- 
- [1] M. Klokkenburg, R. P. A. Dullens, W. K. Kegel, B. H. Erne, and A. P. Philipse, *Phys. Rev. Lett.* **96**, 037203 (2006).
  - [2] M. Klokkenburg, B. H. Erne, J. D. Meeldijk, A. Wiedenmann, A. V. Petukhov, R. P. A. Dullens, and A. P. Philipse, *Phys. Rev. Lett.* **97**, 185702 (2006).
  - [3] B. Reimann, R. Richter, and I. Rehberg, *Phys. Rev. E* **65**, 031504 (2002).
  - [4] J. Richardi, D. Ingert, and M. P. Pileni, *Phys. Rev. E* **66**, 046306 (2002).
  - [5] V. Germain, J. Richardi, D. Ingert, and M. P. Pileni, *J. Phys. Chem. B* **109**, 5541 (2004).
  - [6] Y. Lalatonne, J. Richardi and M. P. Pileni, *Nat. Mat.* **3**, 121 (2004).
  - [7] K. Zahn, R. Lenke, and G. Maret, *Phys. Rev. Lett.* **82**, 2721 (1999).
  - [8] N. Osterman, D. Babic, I. Poberaj, J. Dobnikar, and P. Zihlerl, *Phys. Rev. Lett.* **99**, 248301

- 1  
2  
3 (2007).  
4  
5 [9] O. D. Velev and K. H. Bhatt, *Soft Matter* **2**, 738 (2006).  
6  
7 [10] A. Vorobiev, J. Major, H. Dosch, G. Gordeev, and D. Orlova, *Phys. Rev. Lett.* **93**, 267203  
8  
9 (2004).  
10  
11 [11] J. Jordanovic and S. H. L. Klapp, *Phys. Rev. Lett.* **101**, 038302 (2008).  
12  
13 [12] J. Jordanovic and S. H. L. Klapp, *Phys. Rev. E* **79**, 021405 (2009).  
14  
15 [13] Y. Lalatonne, L. Motte, J. Richardi and M. P. Pileni, *Phys. Rev. E* **71**, 011404 (2005).  
16  
17 [14] J. Richardi, M. P. Pileni, and J.-J. Weis, *Phys. Rev. E* **77**, 061510 (2008).  
18  
19 [15] P. Ilg, *Eur. Phys. J. E* **26**, 169 (2008).  
20  
21 [16] V. A. Froltsov and S. H. L. Klapp, *J. Chem. Phys.* **124**, 134701 (2006).  
22  
23 [17] M. P. Allen and D. J. Tildesley, *Computer Simulation of Liquids* (Academic, London, 1987).  
24  
25 [18] M. Schoen and S. H. L. Klapp, *Reviews in Computational Chemistry*, edited by K. B. Lipkowitz  
26 and T. Cundari (Vol. 24, Wiley-VCH, New Jersey, 2007).  
27  
28 [19] S. H. L. Klapp, Y. Zeng, D. Qu, and R. v. Klitzing, *Phys. Rev. Lett.* **100**, 118303 (2008).  
29  
30 [20] J.-J. Weis, *J. Phys.: Condens. Matter* **15**, S1471 (2003).  
31  
32  
33  
34  
35  
36  
37  
38  
39  
40  
41  
42  
43  
44  
45  
46  
47  
48  
49  
50  
51  
52  
53  
54  
55  
56  
57  
58  
59  
60

## FIGURE CAPTIONS

Figure 1. Zero-field normal pressure as function of the wall separation for three average densities  $\rho^*$  in the Stockmayer system (a)-(c) and the DSS system (d)-(f) at  $\mu^* = 2.0$ . The triangles up (down) indicate where  $\mathbf{H}_z$  ( $\mathbf{H}_{\parallel}$ ) can create (destroy) a layer.

Figure 2. Density profiles at  $H^* = 0$  and in a strong parallel field ( $H_{\parallel}^* = 74$ ) for  $\rho^* = 0.8$  and  $L_z^* = 5.0$  in the Stockmayer system (a) and the DSS system (b).

Figure 3. Intra-layer correlation functions  $g_1^{\text{intra}}(R)$  (contact layer) and interlayer correlation functions  $g_{12}^{\text{inter}}(R)$  between contact layer and the first inner layer at  $H^* = 0$  and in a strong parallel field ( $H_{\parallel}^* = 74$ ) for  $\rho^* = 0.8$  and  $L_z^* = 5.0$  in the Stockmayer system [(a) and (b)] and the DSS system [(c) and (d)].

Figure 4. Density profiles at  $H^* = 0$  and in a strong perpendicular field ( $H_z^* = 74$ ) for  $\rho^* = 0.4$  and  $L_z^* = 5.0$  in the Stockmayer system (a) and the DSS system (b). The insets shows corresponding results at  $\rho^* = 0.6$  (and the same wall separation).

Figure 5. Typical "snapshots" (top view) of SM particles [(a) and (c)] and DSS particles [(b) and (d)] at  $\rho^* = 0.2$ ,  $L_z^* = 5.0$  and two field strengths,  $H_z^* = 7$  [(a) and (b)] and  $H_z^* = 74$  [(c) and (d)]. Also shown are density profiles for the SM (e) and the DSS (f) system at various values of  $H_z^*$  (see labels).

Figure 6. Snapshots (top-view) of SM fluids (upper row) and DSS fluids (bottom row) at  $\rho^* = 0.2$ ,  $L_z^* = 5.0$ ,  $H_z^* = 74$  and different dipolar coupling strengths:  $\lambda = 1$  [(a) and (e)],  $\lambda = 7$  [(b) and (f)],  $\lambda = 10$  [(c) and (g)], and  $\lambda = 20$  [(d) and (h)]. The white circles indicate the positions of particles in the contact layer; black circles correspond to other layers.

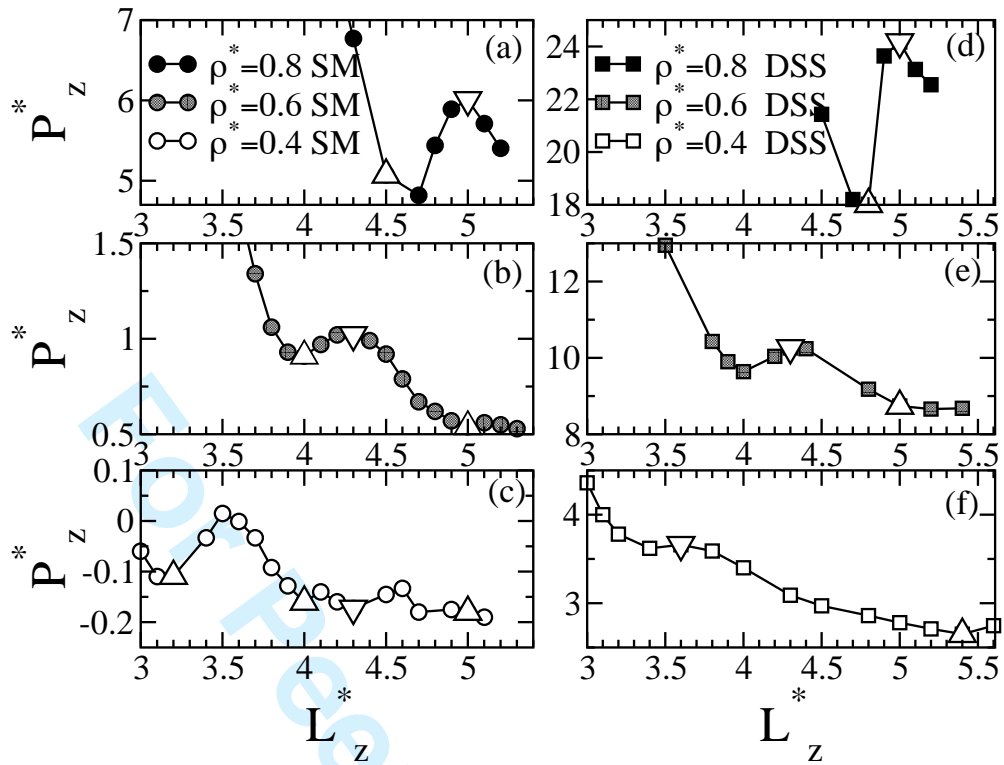
Figure 7. (a) Intra-layer- and (b) interlayer correlation functions in the SM system for various coupling strengths  $\lambda$ . Part (c) shows the behavior of the first peak as function of  $\lambda$ .

1  
2  
3  
4  
5  
6  
7  
8  
9  
10  
11  
12  
13  
14  
15  
16  
17  
18  
19  
20  
21  
22  
23  
24  
25  
26  
27  
28  
29  
30  
31  
32  
33  
34  
35  
36  
37  
38  
39  
40  
41  
42  
43  
44  
45  
46  
47  
48  
49  
50  
51  
52  
53  
54  
55  
56  
57  
58  
59  
60

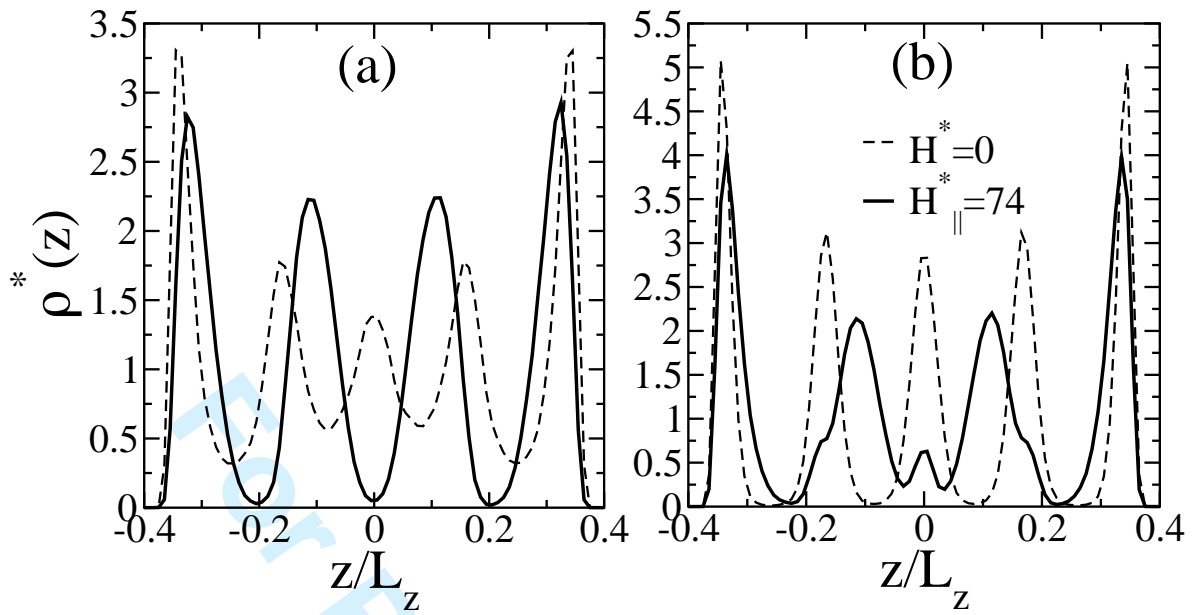
Figure 8. Same as Figure 7, but for the DSS system.

Figure 9. Snapshots at  $\lambda = 20$  and  $H_z^* = 105$ : a) SM system at  $\rho^* = 0.2$ , b) DSS system at  $\rho^* = 0.2$ , c) DSS system at  $\rho^* = 0.1$ . The white circles indicate the positions of particles in the contact layer; black circles correspond to the next (inner) layer.

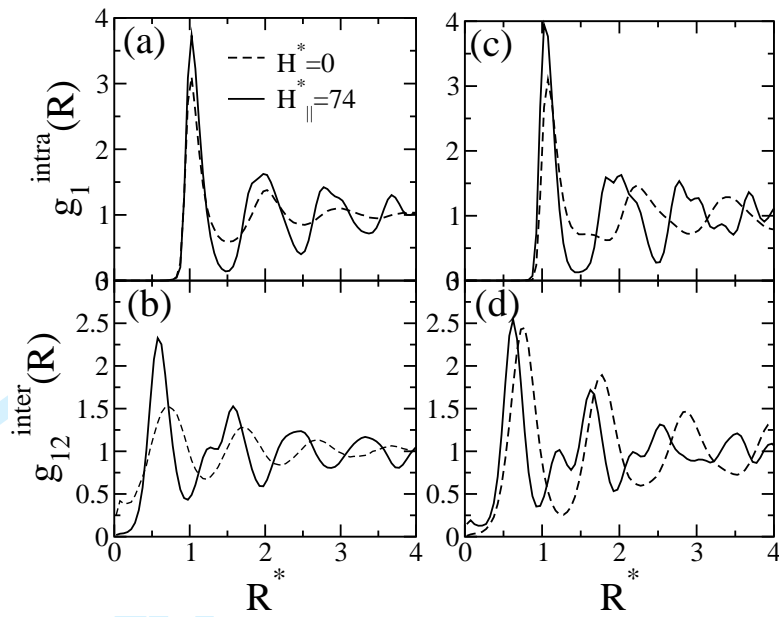
Figure 10. Snapshots (top view) of the contact layer of the SM (a) and the DSS (b) systems at  $\rho^* = 0.2$ ,  $\lambda = 7$ ,  $L_z^* = 5.0$ , and  $H_{\parallel}^* = 74$ . Part (c) shows corresponding density profiles.



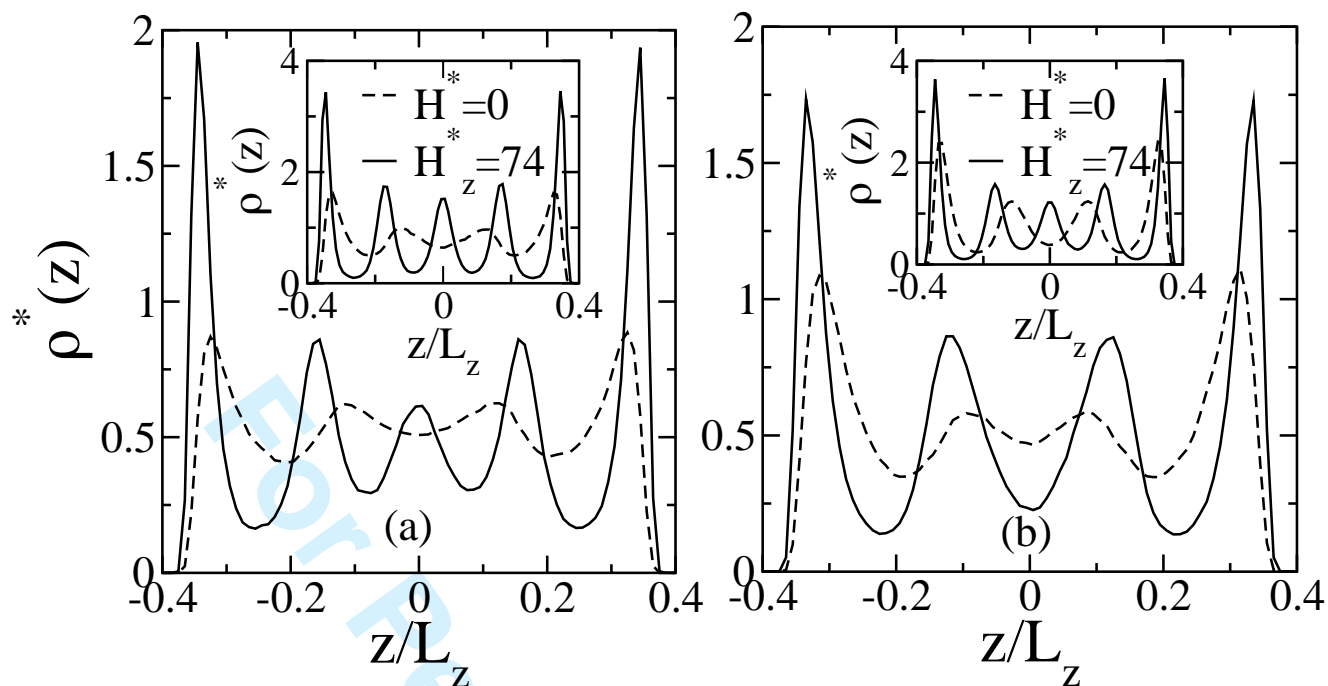
Jordanovic and Klapp, figure 1



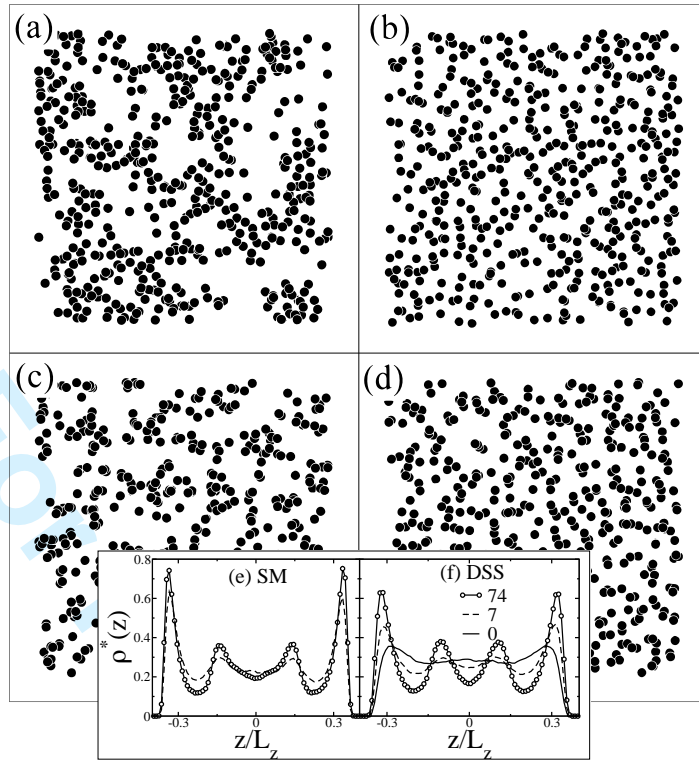
Jordanovic and Klapp, figure 2



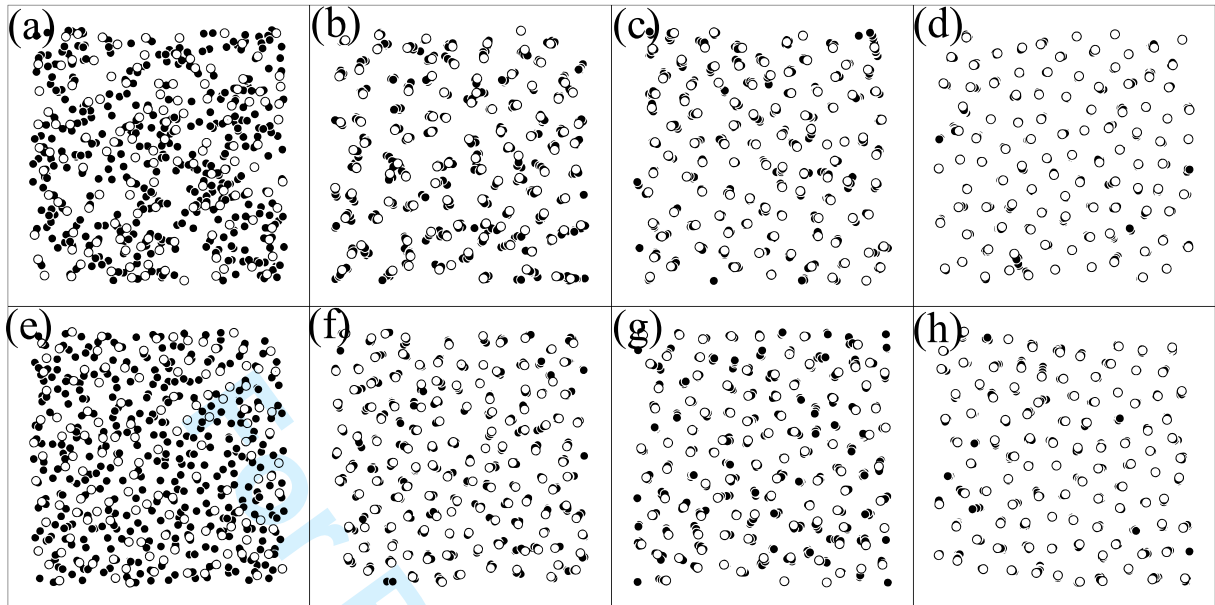
Jordanovic and Klapp, figure 3



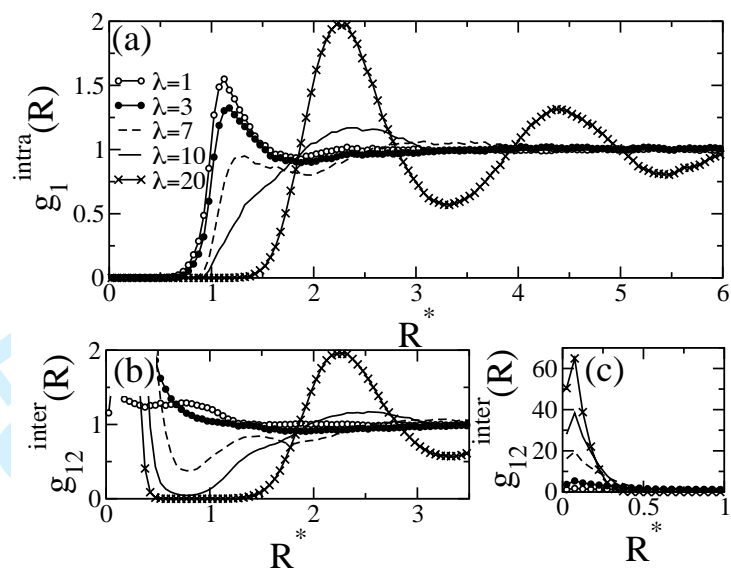
Jordanovic and Klapp, figure 4



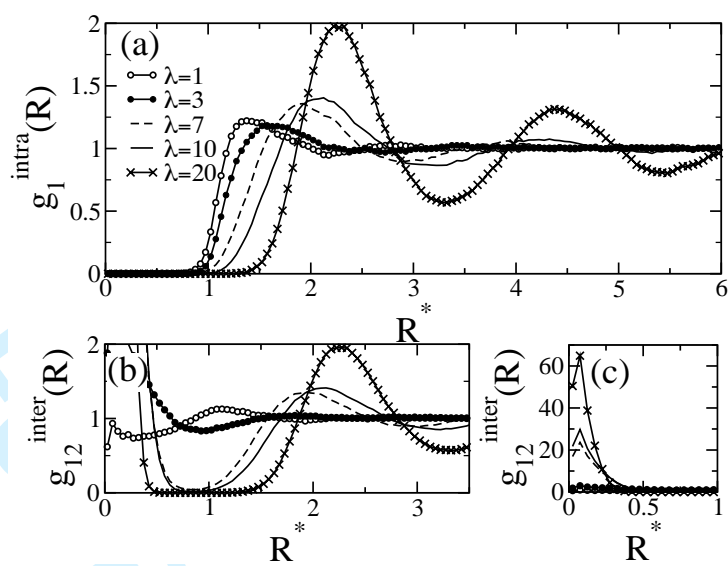
Jordanovic and Klapp, figure 5



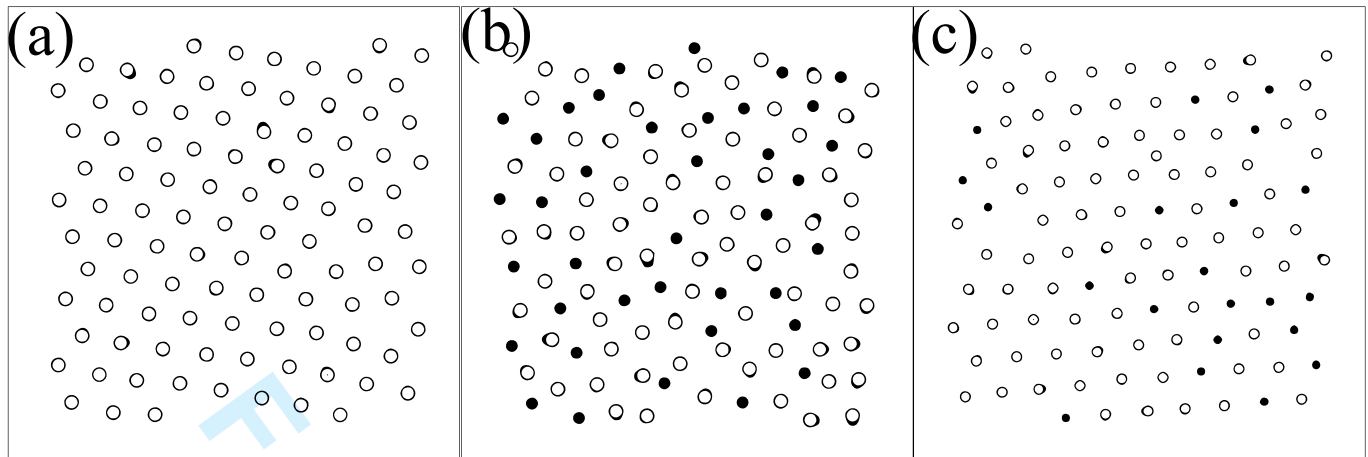
Jordanovic and Klapp, figure 6



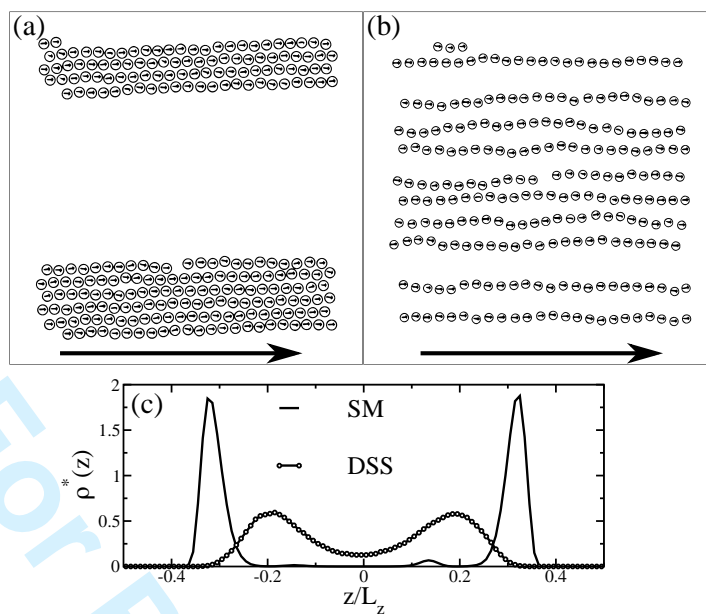
Jordanovic and Klapp, figure 7



Jordanovic and Klapp, figure 8



Jordanovic and Klapp, figure 9



Jordanovic and Klapp, figure 10